HHS Public Access

Author manuscript

J Thorac Cardiovasc Surg. Author manuscript; available in PMC 2021 May 04.

Published in final edited form as:

J Thorac Cardiovasc Surg. 2019 August ; 158(2): 355–363. doi:10.1016/j.jtcvs.2018.10.116.

Pre-Dissection-Derived Geometric and Distensibility Indices Reveal Increased Peak Longitudinal Stress and Stiffness in Patients Sustaining Acute Type A Aortic Dissection: Implications for Predicting Dissection

Leonid Emerel, MD[*,1], **James Thunes, PhD**[*,2], **Trevor Kickliter**[2], **Marie Billaud, PhD**[1,2,4], **Julie A. Phillippi, PhD**[1,2,3,4], **David A. Vorp, PhD**[1,2,3,4,5], **Spandan Maiti, PhD**[2], **Thomas G. Gleason, MD**[1,2,3,4,6]

[1]Department of Cardiothoracic Surgery, University of Pittsburgh, Pittsburgh, PA

[2]Department of Bioengineering, University of Pittsburgh, Pittsburgh, PA

[3]Center for Vascular Remodeling and Regeneration, University of Pittsburgh, Pittsburgh, PA

[4]McGowan Institute for Regenerative Medicine, University of Pittsburgh, Pittsburgh, PA

[5]Department of Chemical & Petroleum Engineering, University of Pittsburgh, Pittsburgh, PA

[6]Center for Thoracic Aortic Disease, University of Pittsburgh, Pittsburgh, PA

Structured Abstract

Objective: To assess ascending aortic distensibility and build geometry and distensibility-based patient-specific stress distribution maps in patients sustaining type A aortic dissection (TAAD) using pre-dissection non-invasive imaging.

Methods: Review of charts from patients undergoing surgical repair of TAAD (n=351) led to the selection of a subset population (n=7) with two or more pre-dissection CTAs and echocardiograms at least one year prior to dissection. Ascending aortic wall biomechanical properties (aortic strain, distensibility and stiffness) were compared to age and size matched non-dissected non-aneurysmal controls. Patient-specific aortic strain served as an input in aortic geometry-based simulated three-dimensional reconstructions to generate longitudinal and circumferential wall stress maps. Inspection of peri-operative dissection scans and intraoperative visual examination confirmed primary tear locations.

Corresponding author: Thomas G. Gleason, MD, Ronald V. Pellegrini Endowed Professor of Cardiothoracic Surgery, Chief, Division of Cardiac Surgery, University of Pittsburgh School of Medicine, Co-Director, UPMC Heart and Vascular Institute, Director, UPMC Center for Thoracic Aortic Disease, Shadyside Medical Building 5200 Centre Ave, Suite 715, Pittsburgh, PA 15232, Phone: 412 802-8529, Fax: 412-647-4710, gleasontg@upmc.edu.

*denotes equal contribution

Disclosures: None

IRB: # PRO07020120

Results: Pre-dissection echocardiography revealed ascending aortas of patients sustaining TAAD to exhibit decreased aortic wall strain (14.50 ± 1.13% vs 8.49 ± 1.08%; $p < 0.01$), decreased distensibility (4.26 ± 0.44 vs 2.39 ± 0.33 $10^{-6}cm^2dyne^{-1}$; $p < 0.01$), increased stiffness (3.84 ± 0.24 vs 7.48 ± 1.05; $p < 0.001$), and increased longitudinal wall stress (246 ± 22 vs 172 ± 37 kPa; $p < 0.01$). There was no significant difference in circumferential wall stress. Pre-dissection CTA models revealed overlap between regions of increased longitudinal wall stress and primary tear sites.

Conclusions: Using pre-dissection imaging, we identified increased stiffness and longitudinal wall stress in ascending aortas of dissection patients. Patient-specific imaging-derived biomechanical property maps like these may be instrumental toward designing better prediction models of aortic dissection potential.

Introduction:

Acute type A aortic dissection (TAAD) is a life-threatening condition initiated by a tear in the intima of the aorta. This tear enables pressurized blood entry into the aortic wall and consequent dissection that can propagate in every direction and compromise vital branch vessel inflow via static or dynamic true lumen compression. Sequelae include acute aortic valve regurgitation, myocardial infarction, stroke, visceral organ ischemia, or frank aortic rupture. Risk factors for dissection include hypertension, bicuspid aortic valve (BAV), and genetically-triggered aortopathies such as the Marfan syndrome (1). If emergent aortic replacement is not performed, aortic dissection is highly lethal (2), and yet our ability to predict aortic dissection is frankly inadequate.

Despite advances in imaging and surgical care, the survival rate following TAAD has seen relatively modest improvements over the years (3) and the factors causing initiation of dissection remain ill-defined. Current guidelines recommend prophylactic surgical replacement of the ascending aorta in non-Marfan patients at an aneurysm diameter of ≥5.5 cm to mitigate the risk of dissection and rupture based on very little data (4). Large retrospective series and data from the International Registry of Acute Aortic Dissection (IRAD) reveal that up to 62% of patients with TAAD have aortic diameters distinctly less than 5.5 cm (5, 6). Thus, aortic size alone is clearly an inadequate predictor of dissection potential. As such, focus has shifted to other potential parameters such as distensibility and wall stress that may help adjudicate risk of dissection (7–9).

From an engineering perspective, dissection is a biomechanical failure of the aortic wall that occurs when ascending aortic aneurysm wall stress exceeds wall strength; thus, wall stress may serve as a reasonable predictor of dissection. Previously, ex-vivo biomechanical failure-testing of ascending aortic aneurysmal tissue specimens allowed for the generation of stress/strain relationships and has improved our understanding of the mechanical properties of aortic aneurysms at the tissue level (10, 11). Computational modeling of ascending aneurysms uncovered differences in longitudinal and circumferential wall stress that correlate with aortic diameter and valve morphology (12–14). However, limitations that restrict the accuracy and validity of these models included both a lack of patient-specific *in vivo* aortic wall biomechanical parameters as model inputs and the clinical knowledge of

whether a dissection actually ever occurred. We hypothesized that patients sustaining TAAD exhibit abnormal aortic wall biomechanical properties prior to the development of dissection, which can be used to generate a computational model and predict wall stress measurements. We focused on the interrogation of patient-specific imaging parameters (aortic geometry and distensibility) from patient's images generated well before they dissected.

Methods:

Cohort selection

All patients undergoing surgical repair of acute TAAD within a single institution were prospectively included in a database and reviewed between 2007–2016 (n=351). All patients identified gave informed consent for chart evaluation and study (IRB # PRO07020120). Inclusion criteria for this study included the presence of a computed tomography angiography (CTA) scan at the time of dissection diagnosis (peri-operative CTA), two or more CTAs obtained at least one year prior to dissection (pre-dissection CTA), and at least one pre-dissection transthoracic echocardiogram. Exclusion criteria included incidence of acute TAAD within one year of a surgical procedure requiring manipulation of the ascending aorta (coronary bypass grafting with proximal aortic anastomosis, aortic valve replacement, or placement of a ventricular assist device) or TAADs caused by retrograde propagation after thoracic aortic endovascular stenting to derive the final cohort (n=7). Control patients (n=7) studied were non-BAV, with no known connective tissue disorder and no prior history of ascending aortic aneurysm, who were matched to the experimental cohort for age and body size (BMI and BSA). Control patients were outpatient referrals seen for evaluation for other conditions who did not undergo surgery. However, it is our policy to also obtain consent from these patients for clinical research purposes.

Identification of intimal tear location

All CTAs at the time of dissection and detailed operative notes from the surgical repairs were reviewed by the senior aortic surgeon (TGG) to identify the primary intimal tear location. Stress maps were derived from computational models by engineers (JT and SM) who were blinded to tear site locations. Tear site locations were compared to stress maps only after completion of all stress maps.

Calculation of aortic strain, distensibility, and stiffness

Aortic elasticity was assessed using the parasternal long axis window of two-dimensional transthoracic echocardiography. Systolic (AoS) and diastolic (AoD) aortic diameters measurements were made 3 cm above the aortic valve annulus; AoD was obtained at the peak of the R wave in the simultaneously recorded electrocardiogram, while AoS was measured at the initiation of the T wave. The following indices of aortic elasticity were calculated as previously described (9, 15, 16):

$$\text{Cardiac cycle aortic wall strain}(\%) = 100\,\frac{\text{AoS}-\text{AoD}}{\text{AoD}}$$

$$\text{Distensibility}\left(10^{-6}\,\text{cm}^2\,.\,\text{dyne}^{-1}\right) = 2\,\frac{\text{AoS}-\text{AoD}}{\text{AoD}\times\text{PP}}$$

$$\text{Stiffness Index} = \frac{\ln(\text{SBP}/\text{DBP})}{\text{AoS}-\text{AoD}}\,\text{AoD}$$

Pulse pressure (PP) was calculated as SBP − DBP, and ln(SBP/DBP) refers to the natural logarithm of the relative pressure. Blood pressure was measured at the time of echocardiography using a cuff sphygmomanometer. Phase 1 and Phase 5 Korotkoff sounds were used for SBP and DBP, respectively. All measurements were made by a single observer with 3–5 measurements per patient, all before the calculation of stain, distensibility, and stiffness indices.

Reconstruction of axial CTA cuts into 3-dimentional images

Aortic geometry was extracted from CTAs using Mimics (Materialize, Leuven, Belgium). Model geometry began near the aortic valve annulus and continued approximately 10–15 cm distal to the aortic arch. Any artifacts in the resulting surface model were removed in Geomagic (3D Systems, Rock Hill, SC). The subsequent blank reconstructions were created in duplicates for each patient and one given to the senior aortic surgeon for primary tear location mapping and one to the engineering team for stress map generation in a blind fashion. The blank engineering model was then meshed with 3-noded triangular elements in Trelis (csimsoft, American Fork, UT). The resulting finite element meshes for the aortic models contained 30,000–50,000 elements to be used for computational model formation (Figure 1).

Patient-specific estimation of aortic wall material parameters

A two-parameter isotropic constitutive model, previously developed by members of our group for abdominal aortic tissue (17), was utilized to simulate biomechanical behavior of the thoracic aortic wall tissue. This model was chosen as a minimally complex constitutive relation capable of capturing the behavior of the tissue. Instead of other popular relations in the literature (18), this model does not include collagen or elastin fiber directions – data impractical for noninvasive clinical measurement. The strain energy density function for the model is given by

$$\Psi = \alpha(I_1 - 3) + \beta(I_1 - 3)^2$$

where $I_1 = \text{tr}\mathbf{C}$ is the first invariant of the right Cauchy-Green deformation tensor, C, and α and β are material parameters. These material parameters were determined in a patient-specific basis by fitting simulated aortic strain to the aortic strain data collected by pre-dissection echocardiography. Individual patient geometries were pressurized to the blood pressure at the time of echocardiography to obtain the simulated aortic strain measured 3 cm above the aortic root. Material parameters (α and β) were modified until the absolute difference between the computationally calculated and clinically measured aortic strain

values were less than 5% from one another. To reduce the potential that a local minima was obtained from the fitting process, 10 initial guesses were used for the parameters. Multiple runs confirmed the uniqueness of the 2 parameters we used.

Finite element simulation and generation of wall stress maps

Wall stress analysis was performed using a custom nonlinear membrane finite element software previously developed by the members of our group (19). The models were constrained against movement at the boundaries of the domain and a pressure of 200 mmHg was applied to the luminal surface of the aorta. Finite element simulations yielded the patient-specific distributions of σ_{LONG} and σ_{CIRC}, the longitudinal and circumferential stresses in the aortic wall tissue, respectively. These stress components were post-processed using Paraview (Kitware, Clifton Park, NY) for visualization purposes. Only the region of interest (ascending aorta) was visually displayed for this paper's objective.

Statistical Methods:

All results mentioned in the text are expressed as mean ± standard error of the mean. Data in Table 1 are expressed as median ± standard error of the mean. Data in Figures 2 and 5 are expressed as individual values. Statistical tests were performed using SigmaPlot, version 12.5 (SYSTAT Software, San Jose, CA). Comparisons between group demographics were assessed by the Mann-Whitney U test. A p value of less than 0.05 was considered statistically significant.

Results:

Patient characteristics

Baseline patient characteristics of both the TAAD and control cohorts are summarized in Table 1. Mean age of the TAAD patient subset was 62.3 ± 3.5 years, with a 5:2 male: female ratio. Mean age of the control patient subset was 61.7 ± 3.5 years, with a 5:2 male: female ratio. All patients in both the TAAD and control cohorts had a morphologically normal tricuspid aortic valve and no history of connective tissue disorders. There were no differences between the two cohorts in age, gender distribution, height, weight, BMI, BSA, SBP, DBP, or PP. Maximum orthogonal diameters were larger among study patients compared to controls (47.8 ± 2.75 mm vs 32.1 ± 1.64 mm; $p < 0.01$). Six of seven (86%) patients in the TAAD cohort exhibited a maximum ascending aortic orthogonal diameter under 5.5cm.

Patients sustaining acute TAAD exhibited abnormal ascending aortic wall biomechanical properties prior to dissection

Pre-dissection aortic systolic diameters, AoS, (4.39 ± 0.23 cm vs 3.61 ± 0.22 cm; $p < 0.05$) and aortic diastolic diameters, AoD, (4.06 ± 0.22 cm vs 3.15 ± 0.18 cm: $p < 0.05$) were increased in study patients compared to controls. Additionally, aortic wall strain during the cardiac cycle (8.49 ± 1.08% vs 14.50 ± 1.13%; $p < 0.01$) and distensibility (2.39 ± 0.33 vs 4.26 ± 0.44 10^{-6}cm^2·dyne^{-1}; $p < 0.01$) were lower when compared with controls, while aortic stiffness indices (7.48 ± 1.05 vs 3.84 ± 0.24; $p < 0.001$) were significantly increased (Figure 2).

Locations of peak longitudinal wall stress overlapped with clinically observed locations of dissection initiation

Circumferential and longitudinal wall stress maps were generated for representative finite element aorta pressurization simulations utilizing aortic strain and geometry (Figure 3). Peak circumferential stress was located on the inner curvature, while peak longitudinal stress was located on the greater curvature of the ascending aorta for the aorta geometries studied. Longitudinal stress maps with surgeon-identified primary tear locations (representative patients shown in Figure 4, overlayed grey regions) were compared to the 95th percentile peak longitudinal wall stress. The peak longitudinal stress in the region of primary tear location was within 10% of calculated peak longitudinal stress in the ascending thoracic aorta on pre-dissection models for all patients studied.

Finite element simulations predicted increased peak longitudinal wall stress for TAAD cohort

Peak longitudinal wall stress for the TAAD cohort was found to be higher than in control patients (246 ± 22 kPa vs 172 ± 37 kPa; $p < 0.01$). There was no significant difference in the peak circumferential wall stress between TAAD patients and controls (Figure 5).

Discussion:

We report the use of pre-dissection echocardiography and CTA to quantify aortic wall biomechanical properties and generate patient-specific pre-dissection stress computational models of the ascending aorta of patients known to later sustain acute TAAD. Our findings reveal that ascending aortas of TAAD patients have decreased strain and distensibility up to more than one year before dissection. Computational stress maps incorporating aortic geometry and echocardiographically-derived aortic distensibility demonstrate that the longitudinal peak aortic wall stress, not the circumferential, is elevated before dissection in the TAAD cohort. Additionally, we found overlap between regions of elevated longitudinal wall stress and the location of primary tears.

These findings corroborate previous investigations that identified aberrant imaging-based aortic wall biomechanics in patient populations with known increased dissection risk such bicuspid aortic valve and Marfan syndrome (7, 16, 20). Others have previously used echocardiography to identify decreased aortic strain and increased stiffness in non-aneurysmal ascending aortas of BAV patients when compared with age- and size-matched controls (9, 21, 22). After adjustment for aortic size and blood pressure, they showed that increased stiffness index positively correlated with aortic diameter (9). Nollen *et al.* prospectively determined aortic stiffness and diameter using magnetic resonance imaging of 78 patients with the Marfan syndrome. They found that decreased ascending aortic distensibility was a major predictor of aortic root dilatation, leading them to conclude that aortic stiffness should be assessed along with standard diameter measurements and growth rate for risk assessment and monitoring of patients with Marfan syndrome (8). Vitarelli *et al.* showed that decreased aortic wall motion and increased stiffness index were independent predictors of aortic dissection among a cohort of 31 Marfan patients (23). Xuan et al. recently reported that both longitudinal and circumferential components of the wall stress

were greater in the ascending aneurysmal aorta of BAV patients compared to TAV patients, and peak stresses were observed at the sinotubular junction (24). Collectively, these reports suggest that a derangement in aortic wall load-bearing properties may be a pre-disposing factor to the increased dissection risk observed in these specific high-risk populations. However, none of these studies utilized pre-dissection images from patients known to dissect.

The landmark study by Rylski et al. investigated the pronounced changes in geometry of the thoracic aorta by the event of aortic dissection, finding an increase in diameter that is most pronounced in the ascending aorta (25). It underscored the critical importance of pre-dissection imaging as the more reliable metric for dissection risk and served as a basis for this work. Although sparse, there has been previously published data on pre-dissection aortic parameters and biomechanics of non-BAV and non-connective disorder patients who ultimately sustained TAAD. Krüger et al. measured ascending aortic length parameters from pre-dissection CTAs in a comparable sized cohort of dissected and non-dissected patients. They found pre-dissected patients to have significantly elongated ascending aortas comparted to non-dissected controls. (26, 27). Yamada *et al.* investigated aortic distensibility in aortic specimens obtained post-dissection using tissue uniaxial testing (28). Interestingly, their histological analysis of the tissue specimens showed decreased elastin content in the dissected cohort, but uniaxial testing suggested increased, rather than decreased, distensibility among patients who sustained dissection (28). No image-based pre-dissection biomechanical assessments were available, and the average age of their cohort was 70 years, significantly higher than seen here. Such findings may further underscore the confounding biomechanical changes that occur in aortic dissection.

Using pre-dissection clinically measured ascending aortic strain and CTA-reconstructed aortic geometry, we generated patient-specific stress/strain models that correlated increased areas of pre-dissection predicted longitudinal stress with primary tear sites at the time of dissection. Finite element simulation and associated biomechanical analysis as a means to assess aortic dissection risk have been previously posited (14, 29–34). However, these prior studies focused on the maximum circumferential stress or stretch as the limiting factor, and the dissection-risk metrics discussed in these studies were devoid of clinical data validation. For example, Beller *et al.* suggested that longitudinal stress, resulting from aortic root motion, was higher in areas of greatest risk of dissection (32). However, this study was performed not on patient-specific, but rather, generalized geometry of the thoracic aorta. In contrast, our multi-parameter and patient-specific stress analysis reveals that only luminal pressure can produce significantly high longitudinal wall stress for dissection patients. We found distinctly that the location of the primary tear site corresponded to regions of predicted peak longitudinal wall stress for all the patients studied. Though there is heterogeneity both along the aorta and about its circumference, the experimental data available to us did not allow for the differentiation of material parameters within aortic layers. However, the elasticity measurements by transthoracic echocardiography along the long axis incorporate all the circumferential layers of the aorta and we would argue is more clinically relevant. Regional variation in the material properties would require a 3D measure of the tissue strains over the cardiac cycle, data not available in a retrospective study such as

this. Though in vivo collection is possible (35) this would be unobtainable in a patient-specific manner during pre-operative risk assessment.

Our results herein support the inclusion of aortic biomechanical parameters into a predictive model of aortic dissection risk. Our next goal is to develop a usable, patient-specific, multi-parameter computational model that includes both cross-sectional imaging and dynamic distensibility indices to better adjudicate aortic dissection potential and to better define more appropriate criteria for surgical intervention.

Limitations:

The number of patients for whom we had multiple pre-dissection CTAs and echocardiograms among a consecutive series of TAADs was small (n = 7) relative to the total cohort mined (n = 351), and consequently may not be representative of the entire TAAD population. We attempted to control for confounding variables and only selected patients that had multiple pre-dissection imaging studies to improve accuracy in wall biomechanics measurements and subsequent stress map generation. Additionally, we did not compare aneurysm patients that did dissect to those that did not. This comparison is the subject of an ongoing study by our group and will be an important component to developing a model that predicts aortic dissection potential.

The distensibility data collected in this study only provided a measure of the wall stiffness in the circumferential direction. Due to the retrospective nature of this study, we chose the location of measurement from previously published work for consistency. We chose not to use the location of maximum aortic diameters as such locations are difficult to identify on transthoracic echocardiography. To that end however, we are currently working on a prospective distensibility study utilizing intraoperative transesophageal echocardiography which will allow for such measurements. For the computational simulations, we assumed that the stiffness in the longitudinal direction was similar to that in the circumferential direction thus motivating our use of an isotropic material model. Our future work will include other methods of distensibility measurements.

Conclusion:

Using a combination of echocardiographic assessment of ascending aortic wall distensibility and CTA-reconstructed stress regional modeling, we generated patient-specific regional stress maps that revealed higher pre-dissection longitudinal wall stress in patients who subsequently sustained TAAD. We show that longitudinal stress should be considered for patient stratification in addition to the usual diameter criterion. In addition, we would also support a higher utilization of aortic elasticity in the assessment of these patients. These findings support using a new, biomechanically-based approach to predicting aortic dissection potential using multiple patient-specific imaging data points. A biomechanically-based paradigm using patient-specific metrics will likely improve our ability to predict aortic dissection potential and thus better direct appropriate elective aortic intervention relative to the current guidelines that are based on maximal orthogonal aortic dimensions.

Acknowledgements

The authors gratefully acknowledge Kristin Valchar, Melissa Enlow and Julie Schreiber for assistance with IRB protocols and informed patient consent as well as image acquisition.

Sources of Funding: Research reported in this publication was supported by the National Heart, Lung and Blood Institute of the National Institutes of Health under award #HL109132 (TGG)

Glossary of Abbreviations

BAV	bicuspid aortic valve
TAAD	type A aortic dissection
CTA	computed tomography angiography
AoS	ascending aortic diameter at peak systole
AoD	ascending aortic diameter at end diastole
SBP	systolic blood pressure
DBP	diastolic blood pressure
PP	pulse pressure
SI	stiffness index
BMI	body mass index
BSA	body surface area
σ_{CIRC}	circumferential stress
σ_{LONG}	longitudinal stress

References

1. Nienaber CA, Clough RE, Sakalihasan N, Suzuki T, Gibbs R, Mussa F, et al. Aortic dissection. Nature Reviews Disease Primers 2016 07/21/online;2:16053.
2. Hirst AE Jr., Johns VJ Jr., Kime SW Jr. Dissecting aneurysm of the aorta: a review of 505 cases. Medicine 1958 Sep;37(3):217–79. [PubMed: 13577293]
3. Trimarchi S, Nienaber CA, Rampoldi V, Myrmel T, Suzuki T, Mehta RH, et al. Contemporary results of surgery in acute type A aortic dissection: The International Registry of Acute Aortic Dissection experience. J Thorac Cardiovasc Surg 2005 Jan;129(1):112–22. [PubMed: 15632832]
4. Erbel R, Aboyans V, Boileau C, Bossone E, Bartolomeo RD, Eggebrecht H, et al. 2014 ESC Guidelines on the diagnosis and treatment of aortic diseasesDocument covering acute and chronic aortic diseases of the thoracic and abdominal aorta of the adultThe Task Force for the Diagnosis and Treatment of Aortic Diseases of the European Society of Cardiology (ESC). European Heart Journal 2014;35(41):2873–926. [PubMed: 25173340]
5. Parish LM, Gorman IIIJH, Kahn S, Plappert T, St. John-Sutton MG, Bavaria JE, et al. Aortic size in acute type A dissection: implications for preventive ascending aortic replacement. European Journal of Cardio-Thoracic Surgery 2009;35(6):941–6. [PubMed: 19237295]
6. Pape LA, Tsai TT, Isselbacher EM, Oh JK, O'Gara PT, Evangelista A, et al. Aortic diameter >or = 5.5 cm is not a good predictor of type A aortic dissection: observations from the International

Registry of Acute Aortic Dissection (IRAD). Circulation 2007 Sep 4;116(10):1120–7. [PubMed: 17709637]

7. Baumgartner D, Baumgartner C, Matyas G, Steinmann B, Loffler-Ragg J, Schermer E, et al. Diagnostic power of aortic elastic properties in young patients with Marfan syndrome. J Thorac Cardiovasc Surg 2005 Apr;129(4):730–9. [PubMed: 15821637]
8. J Nollen G, Groenink M, G P Tijssen J, E Van Der Wall E, Mulder B. Aortic stiffness and diameter predict progressive aortic dilatation in patients with Marfan syndrome; 2004.
9. Nistri S, Grande-Allen J, Noale M, Basso C, Siviero P, Maggi S, et al. Aortic elasticity and size in bicuspid aortic valve syndrome. European Heart Journal 2008;29(4):472–9. [PubMed: 18096569]
10. Pichamuthu JE, Phillippi JA, Cleary DA, Chew DW, Hempel J, Vorp DA, et al. Differential tensile strength and collagen composition in ascending aortic aneurysms by aortic valve phenotype. The Annals of thoracic surgery 2013 Dec;96(6):2147–54. [PubMed: 24021768]
11. Pham T, Martin C, Elefteriades J, Sun W. Biomechanical characterization of ascending aortic aneurysm with concomitant bicuspid aortic valve and bovine aortic arch. Acta biomaterialia 2013 Aug;9(8):7927–36. [PubMed: 23643809]
12. Pasta S, Rinaudo A, Luca A, Pilato M, Scardulla C, Gleason TG, et al. Difference in hemodynamic and wall stress of ascending thoracic aortic aneurysms with bicuspid and tricuspid aortic valve. Journal of biomechanics 2013 Jun 21;46(10):1729–38. [PubMed: 23664314]
13. Viscardi F, Vergara C, Antiga L, Merelli S, Veneziani A, Puppini G, et al. Comparative finite element model analysis of ascending aortic flow in bicuspid and tricuspid aortic valve. Artificial organs 2010 Dec;34(12):1114–20. [PubMed: 20618222]
14. Nathan DP, Xu C, Gorman JH 3rd, Fairman RM, Bavaria JE, Gorman RC, et al. Pathogenesis of acute aortic dissection: a finite element stress analysis. Ann Thorac Surg 2011 Feb;91(2):458–63. [PubMed: 21256291]
15. Ikonomidis I, Lekakis J, Stamatelopoulos K, Markomihelakis N, Kaklamanis PG, Mavrikakis M. Aortic elastic properties and left ventricular diastolic function in patients with Adamantiades-Behcet's disease. Journal of the American College of Cardiology 2004 2004/03/17/;43(6):1075–81.
16. Jeremy RW, Huang H, Hwa J, McCarron H, Hughes CF, Richards JG. Relation between age, arterial distensibility, and aortic dilatation in the Marfan syndrome. The American journal of cardiology 1994 Aug 15;74(4):369–73. [PubMed: 8059700]
17. Raghavan ML, Vorp DA. Toward a biomechanical tool to evaluate rupture potential of abdominal aortic aneurysm: identification of a finite strain constitutive model and evaluation of its applicability. Journal of biomechanics 2000 Apr;33(4):475–82. [PubMed: 10768396]
18. Holzapfel GA, Gasser TC, Ogden RW. A New Constitutive Framework for Arterial Wall Mechanics and a Comparative Study of Material Models. Journal of elasticity and the physical science of solids 2000 2000/07/01;61(1):1–48.
19. Vande Geest J, Bohra A, Sun W, Di Martino E, Sacks MS, Vorp DA. Development and 3D Finite Element Implementation of a Multiaxial Constitutive Relation for Abdominal Aortic Aneurysms. 2004(47039):221–2.
20. Nistri S, Grande-Allen J, Noale M, Basso C, Siviero P, Maggi S, et al. Aortic elasticity and size in bicuspid aortic valve syndrome. Eur Heart J 2008 Feb;29(4):472–9. [PubMed: 18096569]
21. Nistri S, Sorbo MD, Basso C, Thiene G. Bicuspid aortic valve: abnormal aortic elastic properties. The Journal of heart valve disease 2002 May;11(3):369–73; discussion 73–4. [PubMed: 12056729]
22. Alireza M, Mohammad K, Shahnaz S. Aortic distensibility in bicuspid aortic valve patients with normal aortic diameter. Therapeutic Advances in Cardiovascular Disease 2014 2014/08/01;8(4):128–32.
23. Vitarelli A, Conde Y, Cimino E, D'Angeli I, D'Orazio S, Stellato S, et al. Aortic Wall Mechanics in the Marfan Syndrome Assessed by Transesophageal Tissue Doppler Echocardiography. American Journal of Cardiology;97(4):571–7.
24. Xuan Y, Wang Z, Liu R, Haraldsson H, Hope MD, Saloner DA, et al. Wall Stress on Ascending Thoracic Aortic Aneurysms with Bicuspid Compared to Tricuspid Aortic Valve. The Journal of thoracic and cardiovascular surgery 2018.

25. Rylski B, Blanke P, Beyersdorf F, Desai ND, Milewski RK, Siepe M, et al. How does the ascending aorta geometry change when it dissects? J Am Coll Cardiol 2014 Apr 8;63(13):1311–9. [PubMed: 24509277]
26. Krüger T, Oikonomou A, Schibilsky D, Lescan M, Bregel K, Vöhringer L, et al. Aortic elongaLon and the risk for dissecLon: the Tübingen AorLc Pathoanatomy (TAIPAN) project†. European Journal of Cardio-Thoracic Surgery 2017;51(6):1119–26. [PubMed: 28329082]
27. Kruger T, Forkavets O, Veseli K, Lausberg H, Vohringer L, Schneider W, et al. Ascending aortic elongation and the risk of dissection. European journal of cardio-thoracic surgery : official journal of the European Association for Cardio-thoracic Surgery 2016 Aug;50(2):241–7. [PubMed: 26984982]
28. Yamada H, Sakata N, Wada H, Tashiro T, Tayama E. Age-related distensibility and histology of the ascending aorta in elderly patients with acute aortic dissection. Journal of biomechanics 2015 Sep 18;48(12):3267–73. [PubMed: 26163750]
29. Fillinger MF, Raghavan ML, Marra SP, Cronenwett JL, Kennedy FE. In vivo analysis of mechanical wall stress and abdominal aortic aneurysm rupture risk. Journal of vascular surgery 2002 Sep;36(3):589–97. [PubMed: 12218986]
30. Pasta S, Phillippi JA, Tsamis A, D'Amore A, Raffa GM, Pilato M, et al. Constitutive Modeling of Ascending Thoracic Aortic Aneurysms using Microstructural Parameters. Medical engineering & physics 2016 12/06;38(2):121–30. [PubMed: 26669606]
31. Martin C, Sun W, Elefteriades J. Patient-specific finite element analysis of ascending aorta aneurysms. American journal of physiology Heart and circulatory physiology 2015 May 15;308(10):H1306–16. [PubMed: 25770248]
32. Beller CJ, Labrosse MR, Thubrikar MJ, Robicsek F. Role of Aortic Root Motion in the Pathogenesis of Aortic Dissection. Circulation 2004;109(6):763. [PubMed: 14970113]
33. Martin C, Sun W, Pham T, Elefteriades J. Predictive biomechanical analysis of ascending aortic aneurysm rupture potential. Acta biomaterialia 2013 Dec;9(12):9392–400. [PubMed: 23948500]
34. Duprey A, Trabelsi O, Vola M, Favre JP, Avril S. Biaxial rupture properties of ascending thoracic aortic aneurysms. Acta biomaterialia 2016 Sep 15;42:273–85. [PubMed: 27345137]
35. Pasta S, Phillippi J, Gleason T, A Vorp D. Effect of aneurysm on the mechanical dissection properties of the human ascending thoracic aorta; 2011.

Perspective Statement

Little is known about which aortic wall biomechanical abnormalities may pre-dispose to type A aortic dissection. Multi-parameter biomechanical wall stress prediction models could help identify how these properties influence dissection potential and may offer a distinct opportunity for improved risk stratification and management of aortic disease.

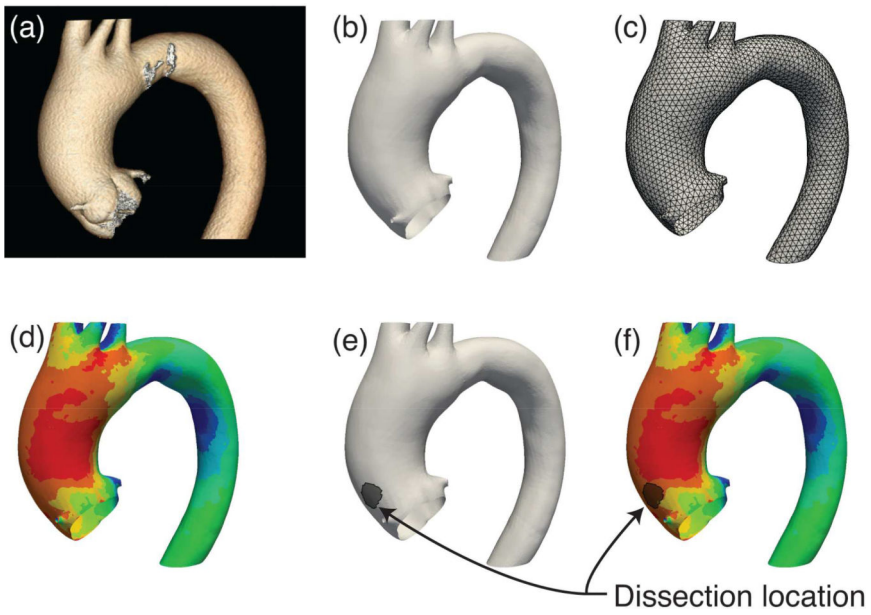

Figure 1: Representative Imaging Reconstruction and Biomechanical Stress Analysis Process.

Patient pre-dissection Computed Tomography Angiography (CTA) scans (a) were reconstructed into 3-dimensional surfaces based on ascending aortic geometry (b), and then discretized for finite element analysis (c). Finite element simulations were performed to obtain longitudinal biomechanical stress contour maps on the aortic wall (d). Clinically observed dissection origins (e) were plotted on the aortic models and were subsequently contrasted against stress contours (f).

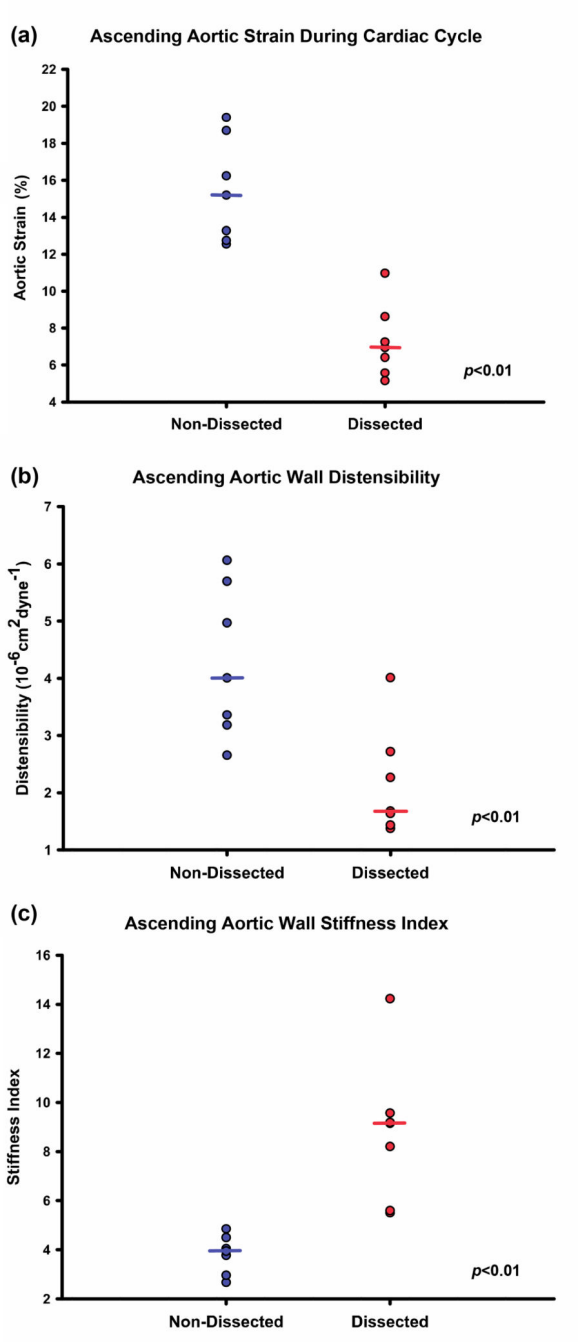

Figure 2: Pre-dissection echocardiography demonstrates aberrant aortic wall biomechanics in patients sustaining type A aortic dissection.

Cardiac cycle aortic strain, distensibility, and stiffness were quantified using transthoracic echocardiography. Dissection patients were found to have decreased aortic wall strain (a) and distensibility (b) and elevated stiffness (c) compared to non-dissected controls. Dot plots indicate individual measurements with horizontal bars serving as the median value.

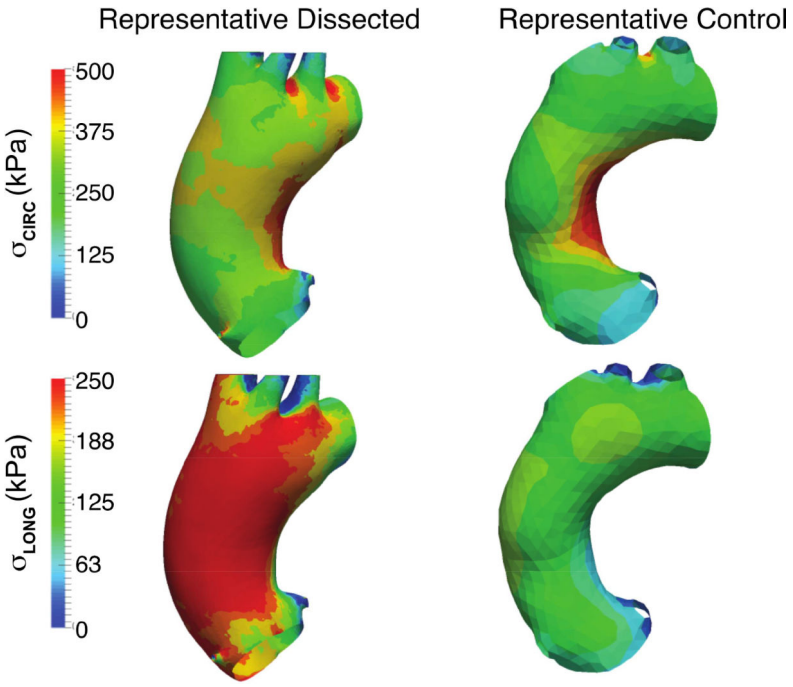

Figure 3: Representative models to demonstrate longitudinal stress is elevated in patients sustaining type A dissection vs. non-dissected matched controls.

Finite element analyses for representative dissected and control aortas after pressurization to 200 mmHg. The top row shows the stress contours in the circumferential direction and the bottom row the stress contours in the longitudinal directions. Magnitudes of circumferential stress is similar between the aortic models while longitudinal stress is significantly higher in the representative dissected aortic model.

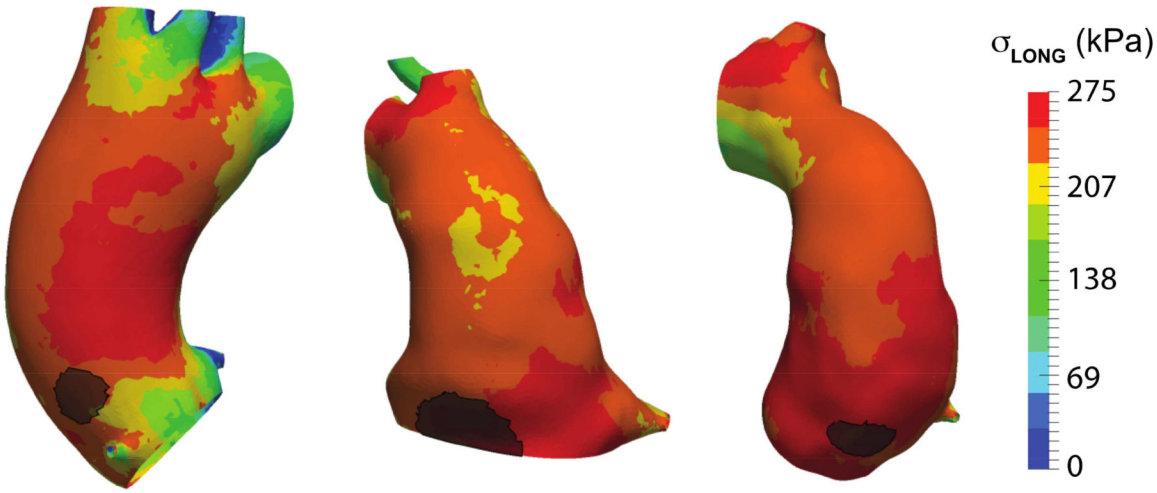

Figure 4: Representative finalized computational models with actual dissection origin overlay.
Ascending aortic longitudinal stress maps of pre-dissection CTAs with the discerned location of dissection as determined by peri-operative CTA overlaid in black.

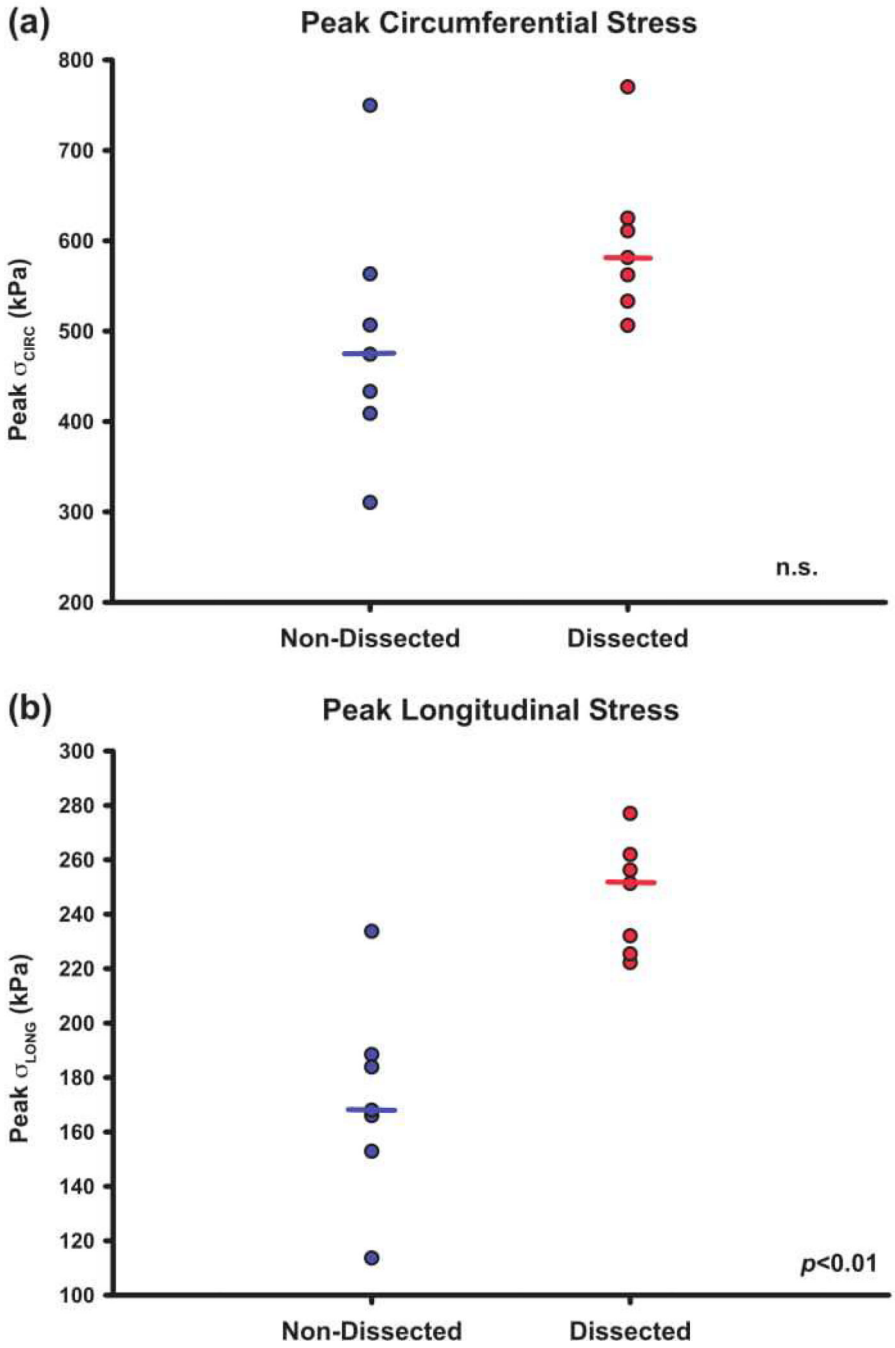

Figure 5: Peak longitudinal stress is elevated in patients sustaining TAAD.

Peak longitudinal stress was quantified using finite element simulation of the computational models. Dissection patients were found to have increased peak longitudinal stress compared to non-dissected controls (a). There was no significant difference in peak circumferential stress between the dissected and control cohorts (b). Dot plots indicate individual measurements with horizontal bars serving as the median value.

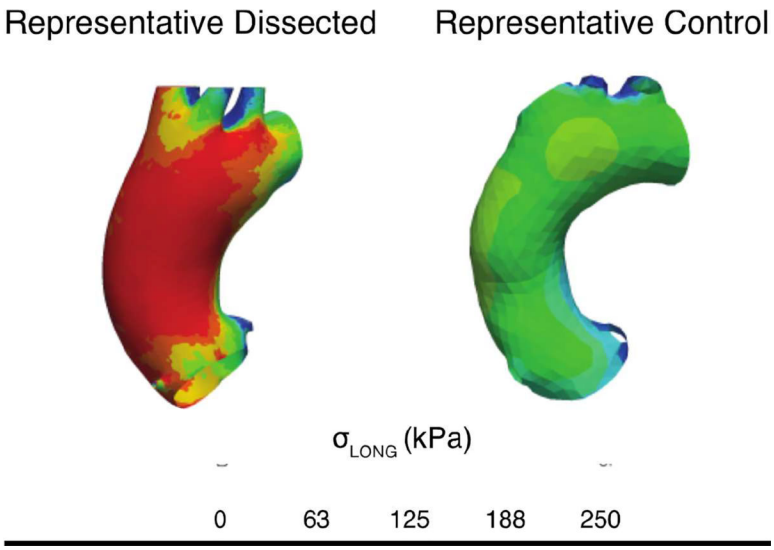

Central Picture. Longitudinal but not circumferential wall stress is elevated in patients sustaining dissection.

Central Message:

Patient-specific ascending aortic wall biomechanical and geometric properties generate wall stress models toward predicting aortic dissection potential.

Table 1:

Baseline Characteristics

	Dissected Cohort (n=7)	Non-Dissected Controls (n=7)	*p* value dissected vs controls
Age (years)	62.25 ± 3.46	61.71 ± 3.52	ns
Sex (% males)	71	71	ns
Height (cm)	175.73 ± 2.98	172.43 ± 3.33	ns
Weight (kg)	88.61 ± 6.78	88.78 ± 9.17	ns
Body Mass Index (kg/m^2)	28.69 ± 2.10	30.98 ± 2.72	ns
Body Surface Area (m^2)	2.04 ± 0.08	2.05 ± 0.10	ns
Maximum Orthogonal Diameter (mm)	47.78 ± 2.75	32.14 ± 1.64	< 0.01
Blood Pressure (mmHg)			
SBP	128.77 ± 7.01	126.88 ± 6.35	ns
DBP	72.78 ± 5.32	71.71 ± 4.54	ns
PP	56.00 ± 5.50	53.75 ± 5.14	ns
AoS (cm)	4.39 ± 0.23	3.61 ± 0.22	< 0.05
AoD (cm)	4.06 ± 0.22	3.15 ± 0.18	< 0.05
AoS-AoD (cm)	0.33 ± 0.03	0.46 ± 0.06	< 0.05
Cardiac Cycle Aortic Wall Strain (%)	8.49 ± 1.08	14.50 ± 1.13	< 0.01
Distensibility ($10^{-6}cm^2dyne^{-1}$)	2.39 ± 0.33	4.26 ± 0.44	< 0.01
Stiffness Index	7.48 ± 1.05	3.84 ± 0.24	< 0.001

Data are expressed as means ± SEM, unless otherwise specified. NS, not statistically significant. p values calculated by Mann-Whitney U test.